Postprint of: Khatami S. M., Naderpour H., Mortezaei A., Maddah M., Lasowicz N., Jankowski R., Optimum shapes and dimensions of rubber bumpers in order to reduce structural pounding during seismic excitations, Structures, Vol. 48 (2023), pp. 1046-1056, DOI: 10.1016/j.istruc.2023.01.026

OPTIMUM SHAPES AND DIMENSIONS OF RUBBER BUMPERS IN ORDER TO REDUCE STRUCTURAL POUNDING DURING SEISMIC EXCITATIONS

Khatami, S.M[1], Naderpour, H[2], Motezaei, A[3], Maddah, M[1], Lasowicz, N[4] and Jankowski, R[4]

[1] University of Applied Science and Technology, Center of Semnan Municipality, Semnan, Iran & Semnan Municipality, Semnan, Iran.
[2]Faculty of Engineering, Semnan University, Semnan, Iran
[3]Seismic Geotechnical and High Performance Concrete Research Centre, Civil Engineering Department, Semnan Branch, Islamic Azad University, Semnan, Iran
[4]Faculty of Civil and Environmental Engineering, Gdansk University of Technology, Gdansk, Poland

Corresponding author: Natalia Lasowicz
E-mail: *natmajew@pg.edu.pl*

ABSTRACT

Large displacement of structures observed during seismic excitations may lead to collisions between two adjacent, insufficiently-separated buildings and may result in major damages of both of them. In many building codes, appropriate equations or approximately recommended distances between structures in order to avoid pounding hazard have been introduced. Unfortunately, further, more detailed considerations show that safety situation or economic aspects are not always satisfied due to the collisions between buildings and the cost of land, respectively. Hence, researchers have studied other approaches of reducing the negative pounding effects. Such methods include the use of tuned mass or liquid dampers. Moreover the increase in stiffness of building or reduction of mass of the structure are still considered. In this paper, another approach is considered by the application of rubber bumpers placed between buildings. The bumpers are attached at each story to absorb energy during impact. Several different shapes and dimensions of bumper elements were numerically investigated so as to find the most effective ones most effective in reducing structural pounding negative effects. For this purpose, two MDOF models of 3-story and 4-story buildings were firstly considered. Such parameters as lateral displacement, damage index, dissipated energy and impact forces were calculated and depicted as the results of numerical study. Then, different shapes and dimensions of bumpers were parametrically investigated.

Key words: structural pounding; rubber bumpers; seismic excitations

1. INTRODUTION

Seismic excitations may cause unpredictable and dangerous situations for structures [1,2]. One of the threats is related to collisions between neighbouring buildings or bridge segments [3-5,6]. Such collisions, often referred as structural pounding, are observed when adjacent structures, or structural elements, are constructed very close to each other without the adequate in-between distance. In order to avoid impact incidents during seismic excitations, or reduce their negative effects, different approaches can be applied. In the case of buildings, the most natural solution is to provide sufficiently large separation distance between structures [7,8]. However, this approach may not be always accepted due to the cost of land in the case of many metropolitan cities. Therefore, other solutions focused on reducing the gap distance between buildings and still preventing pounding during earthquakes, were studied. Anagnostopolos and Karamaneas [3], as well as Barros and Khatami [9] numerically investigated the effectiveness of concrete shear wall to increase stiffness of buildings and control their lateral displacements. Dogrul [10], Barros and

Braz [11] and Garcia [12,13] focused on nonlinear behavior of structures to decrease lateral displacement by using passive dampers and also presented the genetic algorithms for optimal seismic design of passively damped structures. Zhang and Xu [14], as well as Matsagar and Jangid [15] investigated the linkage of adjacent structures with spring and dashpot to decline relative displacement of structures. Connection between adjacent buildings by using additional stiff beams in order to absorb energy was evaluated by Westermo [16]. Kasai et al [17] eliminated pounding effects by applying viscoelastic dampers between buildings [18]. Different approaches to control structural deformations are related to the use of base isolation, which is considered to be one of the most effective methods of improving the seismic response of structures (see, for example, Kelly [19], Falborski et al [20,21], Jankowski [22] and Liu et al [23,24]). It should be underlined, however, that the approach results in the increased absolute structural displacements with relation to the ground, increasing also the probability of pounding between buildings during earthquakes [25]. The excessive displacements can be somehow controlled by additional dampers (see, for example, Naderpour et al [26] and Zhao et al [27]) but still it may not be enough to prevent collisions between isolated structures.

Another method to reduce negative effects of collisions is to use rubber bumpers, attached at the level of each story so as to dissipate energy during impact (see Panayiotis et al [28], Anagnostopolos [29], Polycarpou et al [30] and Raheem [31], Khatami et all [32], Al-Fahdawi et al [33,34] and Matsagar et all [35], Sołtysik and Jankowski [36]). The aim of current study is to consider the most effective shape, plan dimensions and thickness of a rubber bumper to absorb energy between adjacent structures during collision when displacements of them are exceeded from their limitations. For this purpose, one 3-story and one 4-story dynamic models have been created and analysed. Both models have been described by the same mass, stiffness and damping ratio of each story. Moreover, rubber bumpers have been attached in the place of contact zone in order to investigate the effect of different shapes, plan dimensions and thicknesses.

2. SIMULATION OF BUMPERS

Rubber bumpers are those type of elements, that are attached at the contact area of two adjacent building to control impact and dissipated energy during seismic excitations. Special type of material, shape, plan dimension and thickness are the most important parameters in the field of impact when rubber bumpers are used. Since the behaviour of rubber bumpers significantly depends on their dimensions and shape, Jankowski et al [37] have basically presented a linear spring to perform as rubber bumper which shows a stiffness value as the below:

$$k_{linear} = \frac{A.E_r}{t} \tag{1}$$

where A, E_r and t are contact area, Young modulus and the thickness of bumper, respectively. When buildings show nonlinear behaviour during earthquake, linear model is not able to present complete response when bumpers are activated. Consequently, stiffness of spring is expressed by:

$$k_{imp} = \frac{A.k_r}{t^n} \tag{2}$$

In here, k_r denotes the material stiffness and n is the exponent to show nonlinear behaviour of bumpers. In order to simulate impact and calibrate the results of numerical analyses, an impact relation is used based on two different approaches, which are defined as:

$$F_{imp} = \begin{cases} k_{imp}.\delta^n \rightarrow \dot{\delta} > 0 \\ k_{imp}.\delta^n.(1+[1.55\dfrac{(1-(\dot{\delta}_{imp}/\dot{\delta}_{rebound})^2)}{(\dot{\delta}_{imp}/\dot{\delta}_{rebound})^{0.7076}}].\dot{\delta}) \rightarrow \dot{\delta} < 0 \end{cases} \quad (3)$$

where k_{imp}, δ and $\dot{\delta}$ are the the initial impact stiffness, deformation of colliding structural members and relative velocity between them; while $\dot{\delta}_{imp}$ and $\dot{\delta}_{rebound}$ denote the prior-impact and post-impact relative velocities. Based on equation (3) and for the first phase when $\dot{\delta} > 0$, a value of 80% of the thickness of rubber bumper is estimated to be the ultimate value of indentation, which are expressed by:

$$F_{imp} = \begin{cases} k_{imp}.\delta^n \rightarrow \delta < \delta_u \\ k_{imp}.\delta_u^n + k_w(\delta - \delta_u) \rightarrow \delta > \delta_u \end{cases} \quad (4)$$

where δ_u is ultimate relative deformation and k_w stands for the linear post yield impact stiffness.

The CRVK program has been used to perform dynamic model of buildings with different number of stories, mass, stiffness and other building parameters, earthquake record and the properties of rubber bumpers, and also analyse, solve and show impact during seismic excitation. The CRVK program was designed and written by Khatami et al at [38] together with Faculty of Engineering of the University of Porto (FEUP) for modelling various buildings with different properties and makes several matrixes to solve mathematical relations for getting responses based on input data. Numerical model has been calibrated based on the previously conducted experimental study by Katija et al [39], where impact test between two steel rods by using a 300 kg mass for each bodies have been conducted. One rubber bumper with square shape, plan dimensions 4x4 cm and thickness of about 1 cm was modelled. An impact velocity was assumed to be 0.68 m/s based on the results of experiment test conducted by Katija et al [39]. Using equation (3) and artificial neural network (applying CRVK program), the analyses were carried out and all inputs from experimental test were collected, including mass, dimensions and the results of the test (displacements, impact forces, test time). Then program conducts an iterative process between input and output, saves the data and trains all inputs to receive the optimum results. The effectiveness of the training, testing and validation of the solution is larger than 97% which shows the accuracy of the approach. The results of the model calibration are presented in Figure 1a and 1b.

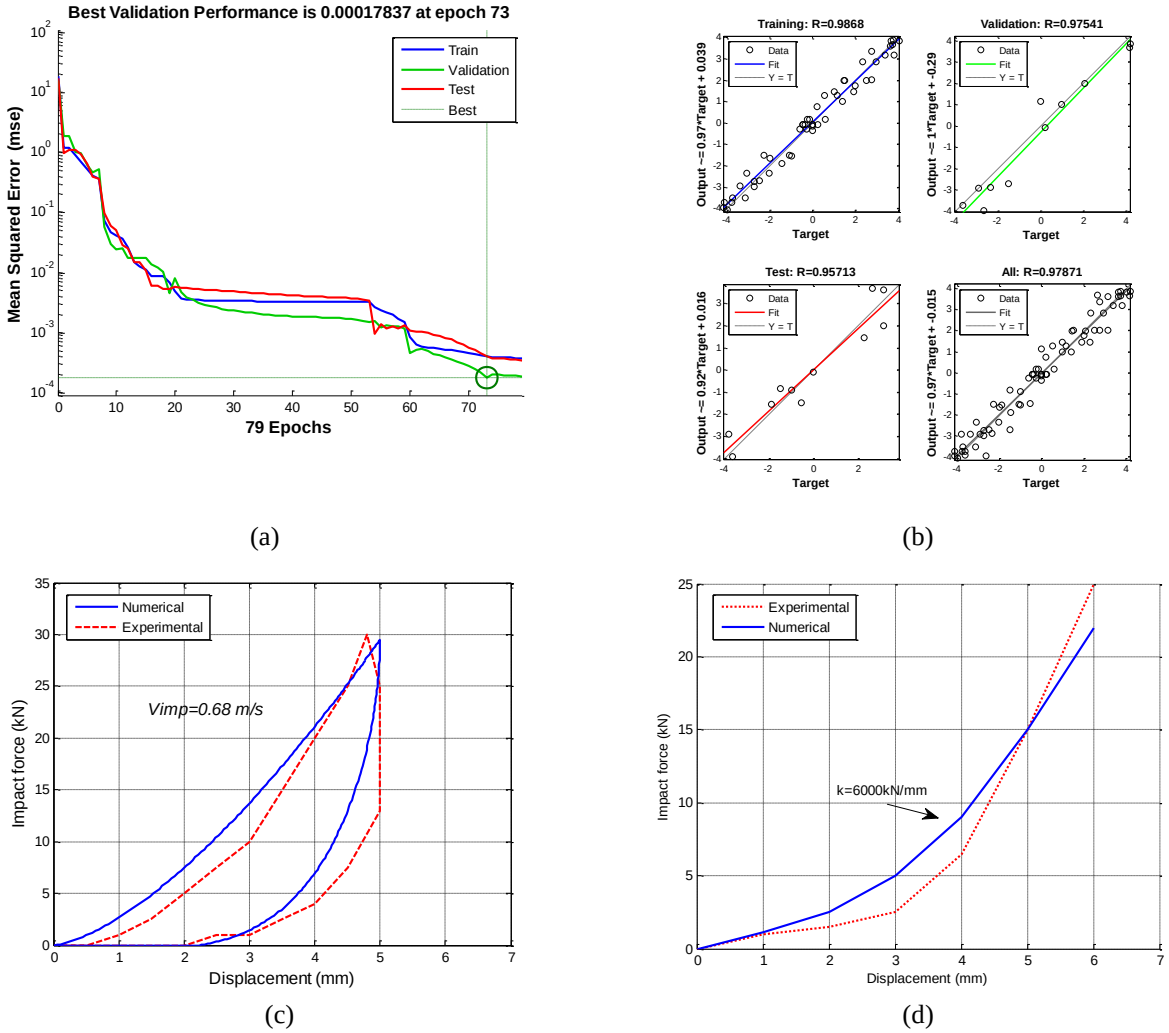

Figure 1. The results of model calibration: a) results of validation test; b) details of artificial neural network analyses; c) hysteresis curve; d) static analyses.

As it can be seen in Figure 1d, maximum impact force determined from experimental test was 25 kN, while in the case of numerical analysis it was equal to 21.9 kN, which shows 13% of error in static analysis. On the other hand, CRVK program has demonstrated calibrated response in zone of hysteresis curve by showing 30 kN impact force, which is equal to the results of experimental test with same final displacement of about 5 mm (see Figure 1c). The value of dissipated energy is calculated to be 43.23 kN·mm and 39.85 kN.mm for experimental and numerical responses, respectively. The results of calibration have obviously shown an accepted accuracy of using CRVK program.

3. NUMERICAL STUDY

In order to investigate the effect of rubber bumper and introduce the optimum plan dimensions, thickness and also the best shape so as to absorb energy, two concrete buildings (one 3-story and one 4-story), located with 10 cm distance from each other, were analysed. The following dimensions (length x width x height) of the buildings were specified: 6.5x6.5x9 m and 6.5x5x12 m, for the 3-story and 4-story structure, respectively. Columns and beams were considered as the

major structural elements of both buildings. In the case of 3-story structure, the columns' cross-section was taken to be 30x30 cm, while, in the case of 4-story building, it was 35x35 cm. Moreover, the square cross-section of beams (30x30 cm) was considered in both structures. Soil parameters were taken to be the same for both buildings. The lumped-mass model of 3-story building had the story mass of 44700 kg, the story lateral stiffness of 450 MN/m, the natural vibration period of 1.4 s (frequency of 1/1.4 = 0.71 Hz), the damping ratio of 5%. On the other hand, the lumped-mass model of 4-story building was described by the following parameters: the story mass of 26500 kg, the story lateral stiffness of 350 MN/m, the natural vibration period of 1.22 s (frequency of 1/1.22 = 0.82 Hz), the damping ratio of 5%. Initial stiffness and post yield stiffness of isolation system were assumed to be 40 MN/m and 5 MN/m, what described the bilinear characteristics of the isolation system. First model was assumed to be 4-story model with previously mentioned properties while second model is 3- story model. The 3-story structure was additionally equipped with three square bumpers. Those elements were placed at the contact zone of each story of the building and the scheme of their arrangement is presented in Figure 2. Rubber bumpers were used to control impact force and absorb energy during collisions. They were modelled based on a square plan section with 25x25 cm plan dimensions and 5 cm of thickness. The stiffness of bumpers was assumed to be equal to 0.12 kN/mm, while the post yield impact stiffness was considered to be 500 kN/mm. The cross-sectional area of the bumper was equal to 625 cm^2 and also the volume of each bumper was calculated to be 3125 cm^3. In this study a rubber bumper described by such dimensions was assumed to be the reference one. Secondly, different plan dimensions and thicknesses of bumpers were investigated keeping the same volume. It should be underlined that thickness that significantly depends on gap size between models (10 cm) had to be limited to this value.

A number of different earthquake records were applied in the analysis. The acceleration time histories measured during the real seismic events, as well as the spectrum-matched ground motions (see [40, 41], for example), were considered. However, in this paper, the most representative results are presented, which were obtained for the well-known El Centro 1940 earthquake (peak ground acceleration of 307 cm/s^2, magnitude of 6.9 in the Richter scale). This earthquake record is characterized by a wide range of dominant frequencies and it is often used in earthquake engineering [42].

The effect of using different values of thickness was evaluated keeping the same pounding involved response impact and dissipated energy. It was also mentioned that the effect of thickness was considered based on the same contact area. Finally, the main assumption was to keep the same volume with different value of plan dimensions and thickness. The final evaluation was focused on determining the optimum shape of rubber bumper.

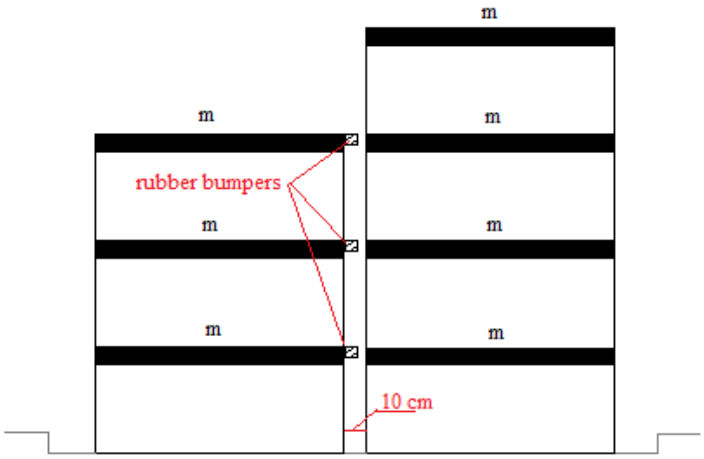

Figure 2. Arrangement scheme of rubber bumpers placed on 3-story model of building.

In order to investigate the effect of plan dimensions of bumpers, the reference model was numerically analysed and lateral displacements of both models of buildings were separately depicted in order to compare them with each other. In Figure 3, the lateral displacement time histories of each story of 4-story model (Figure 3a) and 3-story model (Figure 3b) are presented. It can be seen from the figure that the peak value of displacement for the 3rd story is equal to 19.1 cm and 16.3 cm for 4-story and 3-story model, respectively. Since the 3rd story is the top one in the case of the lower building, further results for this story of both models are presented in Figure 4.

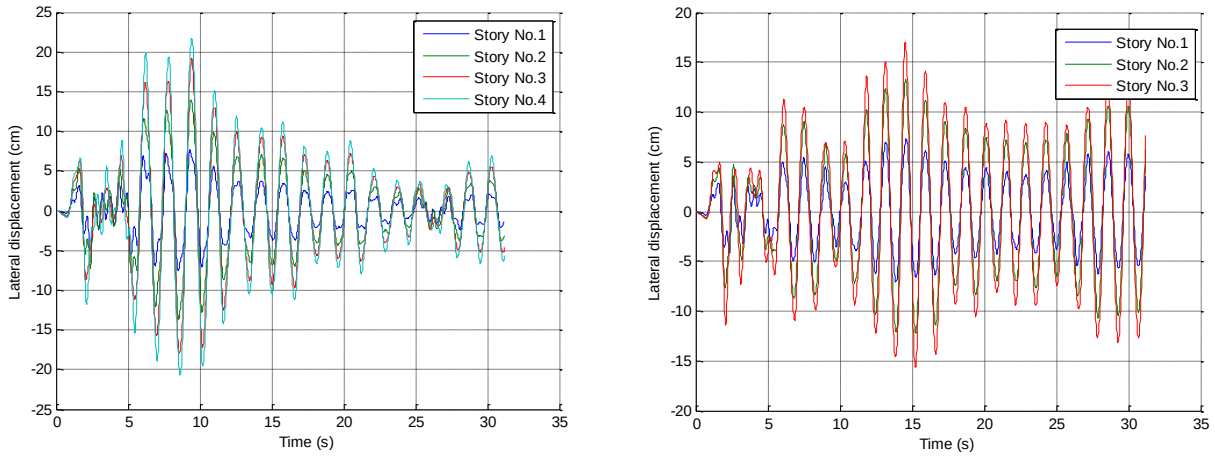

(a) (b)

Figure 3. Lateral displacement time histories determined for all stories of: a) 4-story model of building; b) 3-story model of building.

As it can be seen from Figure 4a, some collisions during seismic excitation were observed. The maximum values of relative lateral displacement between models significantly exceeded initial in-between distance of 10 cm what means that it is an insufficient gap size and cannot protect buildings against impacts. Consequently, rubber bumpers were automatically activated to dissipate energy in order to decrease destructive effect of earthquake. In Figure 4b a hysteresis

curve of rubber bumper is presented. The maximum value of impact force was demonstrated to be $3.88 \cdot 10^{11}$ kN for story no.3, while the maximum calculated value of absorb energy was equal to $28.26 \cdot 10^{11}$ kN·cm.

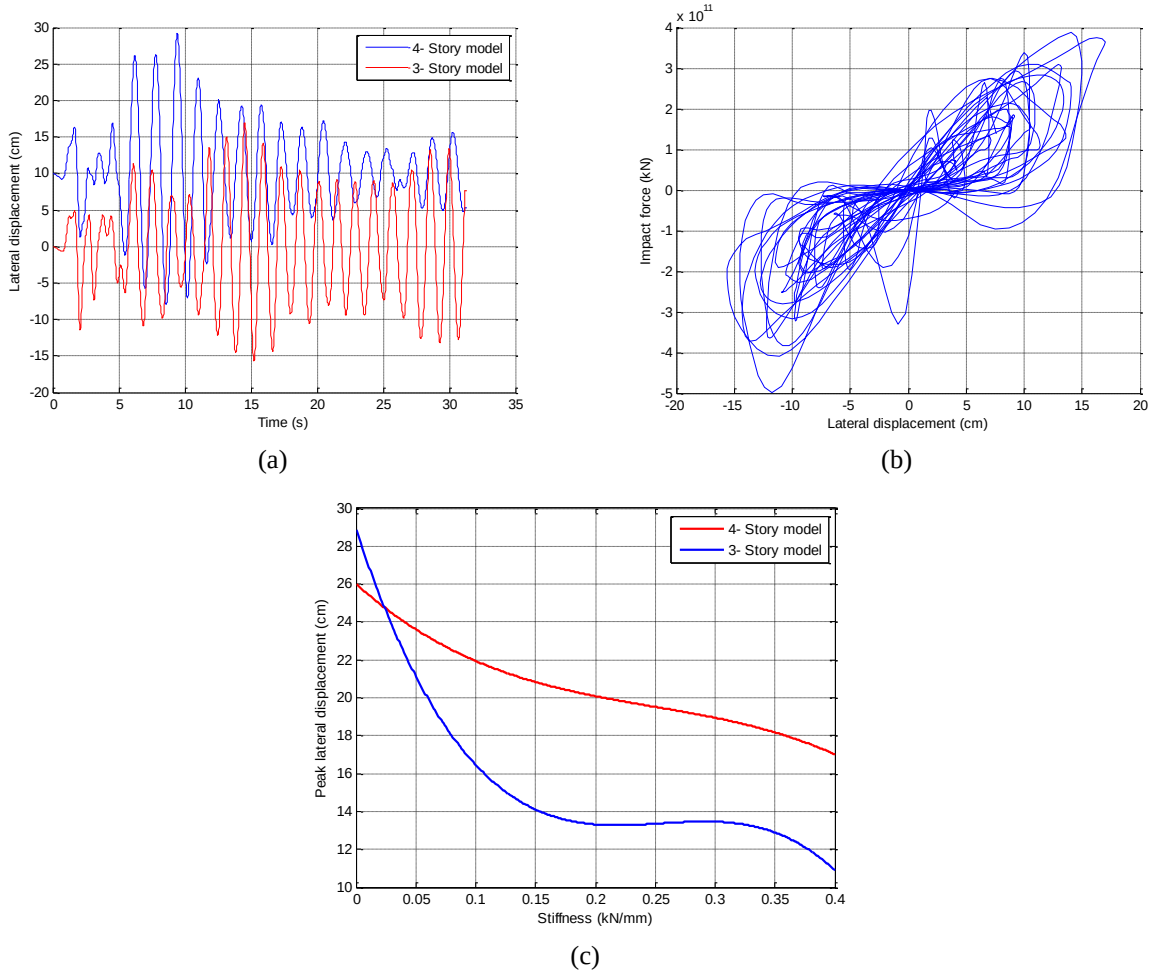

Figure 4. a) Lateral displacement time history of story no.3 of both models; b) hysteresis curve of rubber bumper; c) peak lateral displacement of both models under El Centro earthquake record.

As it can be seen in Figure 4c, increasing the value of stiffness of bumpers, peak lateral displacements determined at story no. 3 of both models are slightly decreased for 4-story model and also sharply declined for 3-story model. It shows that rubber bumpers are able to control and reduce the peak lateral displacement of buildings that are equipped with them and also they are able to indicate normal behaviour (increase or decrease) for the adjacent building without rubber bumpers.

3.1 Rubber bumpers characterized by the same volume but different plan dimensions

Further step of investigation was focused on bumpers that were characterized by the same volume but different plan dimensions and thicknesses. They were selected in order to obtain hysteresis loops and then were compared with the results determined for reference model. Similar response in zone of impact force and energy dissipation was considered as main assumption to find optimum dimension of bumpers. For this challenge, five following different

dimensions of square bumpers with the same volume were considered: 17.7x17.7x10 cm, 20x20x7.8 cm, 25x25x5 cm, 30x30x3.45 cm and 35x35x2.55 cm. The hysteresis loop of different value of dimension of bumpers characterized by the same volume but different plan dimensions are presented in Figure 5.

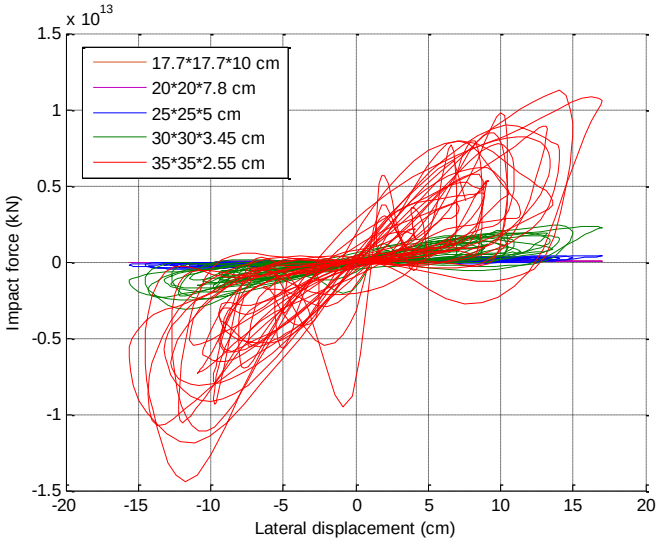

Figure 5. Hysteresis loop of bumpers with the same volume but different plan dimensions.

The maximum impact forces determined from the analysis were equal to: $1.23 \cdot 10^{10}$ kN, $4.17 \cdot 10^{10}$ kN, $3.88 \cdot 10^{11}$ kN, $2.4 \cdot 10^{12}$ kN and finally, $1.12 \cdot 10^{12}$ kN for the following dimensions of bumpers: 17.7x17.7x10 cm, 20x20x7.8 cm, 25x25x5 cm, 30x30x3.45 cm, 35x35x2.55 cm, respectively. The maximum dissipated energies obtained from the study were equal to: $9.08 \cdot 10^{10}$ kN.cm, $30.87 \cdot 10^{10}$ kN.cm, $8.26 \cdot 10^{11}$ kN.cm, $17.72 \cdot 10^{12}$ kN.cm and $8.29 \cdot 10^{13}$ kN.cm, respectively.

It seems that by increasing the value of bumper thickness, impact force and dissipated energy basically decrease. In fact, the same volume of bumpers has specifically shown various responses in field of impact force and energy dissipation. For instance, when the thickness is declined by about 75%, impact force and dissipated energy suddenly grown about 910 times compared to reference model.

3.2 Rubber bumpers characterized by the same responses but different dimensions

Second round of investigation was focused on determining such dimension and shape of rubber bumpers so as to estimate similar responses in zone of impact force and also dissipated energy. In here, plan dimensions of square shape of bumpers analysed in a previous part (see section 3.1) were introduced, only value of thicknesses were changed in order to calibrate hysteresis responses with reference model. Following plan dimensions of square shape of bumpers have been analysed: 17.7x17.7 cm, 20x20 cm, 25x28 cm, 30x30 cm and finally, 35x35 cm of thickness 3.15 cm, 3.7 cm, 5 cm, 6.4 cm and finally, 7.8 cm, respectively. The hysteresis loop of bumpers characterized by the same response during impact but different plan dimensions and thicknesses are presented in Figure 6. The results of investigation demonstrate that by increasing the value of plan dimensions of square shape bumpers, the value of thickness is increased to obtain similar responses during impact between models.

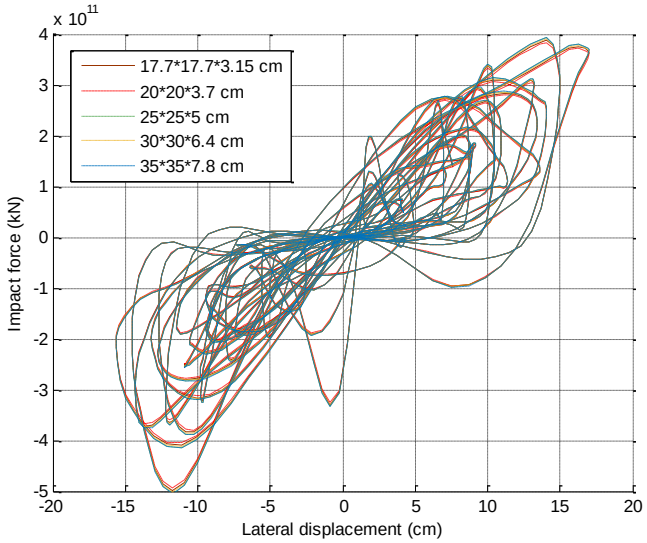

Figure 6. Hysteresis loop of bumpers with different plan dimensions and thicknesses but the same response during impact.

3.3 Rubber bumpers characterized by the same cross-sectional area but different thickness

Third part was performed to evaluate the influence of thickness on dissipate energy and impact force. For this purpose, reference model that was previously assumed with plan dimension 25x25 cm was analysed with different value of thicknesses such as 1 cm, 2.5 cm, 5 cm, 7.5 cm and 10 cm. The area of all considered bumpers was equal to 625 cm^2 and then their volumes were calculated and were equal to 625 cm^3, 1562 cm^3, 3125 cm^3, 4687 cm^3 and 6250 cm^3 for bumper of thickness 1 cm, 2.5 cm, 5 cm, 7.5 cm and 10 cm respectively. In Figure 7 hysteresis loop of rubber bumpers characterized by the same cross-sectional area but different volume are presented.

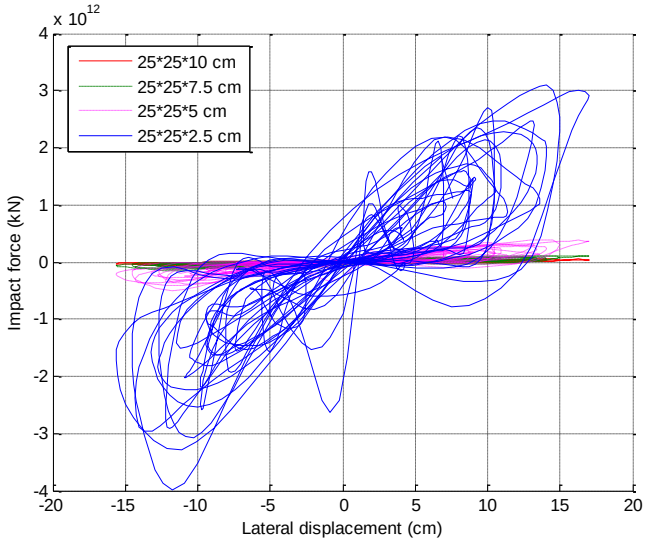

Figure 7. Hysteresis loop of rubber bumpers with the same cross-sectional area (25*25 cm) but different volume.

As it can be seen from Figure 7, the maximum impact forces were equal to: $4.85 \cdot 10^{10}$ kN, $1.10 \cdot 10^{11}$ kN, $3.44 \cdot 10^{11}$ kN and finally, $3.14 \cdot 10^{12}$ kN for bumper of thickness 10 cm, 7.5 cm, 5 cm and finally, 2.5 cm, respectively. It shows, that by decreasing the thickness of bumpers, impact force and dissipated energy significantly increased.

3.4 Rubber bumpers characterized by the same plan dimensions but different shapes

Another consideration was focused on different shapes of rubber bumper. Firstly, a bumper of a circle shape and the same dimension as reference model (with square shape) was selected. That's why bumper of circle shape with diameter equal to r=12.5 cm (d=25 cm) was assumed so as to keep the same response with reference model. The thickness of circle model was assumed 1.65 cm in order to provide similar response with square model. It can be calculated that the volume of square and circle model is 3125 cm^3 and 810 cm^3, respectively.

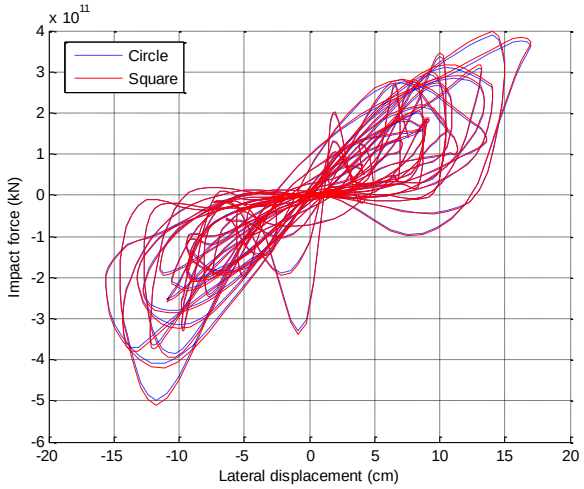

Figure 8. Hysteresis loop of bumper with same dimensions but different shapes.

As it can be seen in Figure 8 square model has shown similar response compared to circle one when the volume of bumper is 4 times greater than circle model. It seems that using circle shape of bumper has an effective role in zone of economy situation as the used material is suddenly declined about 75%.

3.5 Rubber bumpers characterized by the same cross-sectional area but different shapes

On the other hand, same contact area was assumed to compare the results of investigation. In here, square shape model with cross-sectional area equal to 625 cm^2, which in the case of circle one results in radius around r=14.1 cm. In order to perform dynamic analyses and similar response, circle model should be considered of at thickness of about 1.95 cm. Figure 9 shows hysteresis loop of bumper with the same contact area, similar responses but different shapes. The volume of the newly created model was 1217 cm^3, that was 61% less than square one.

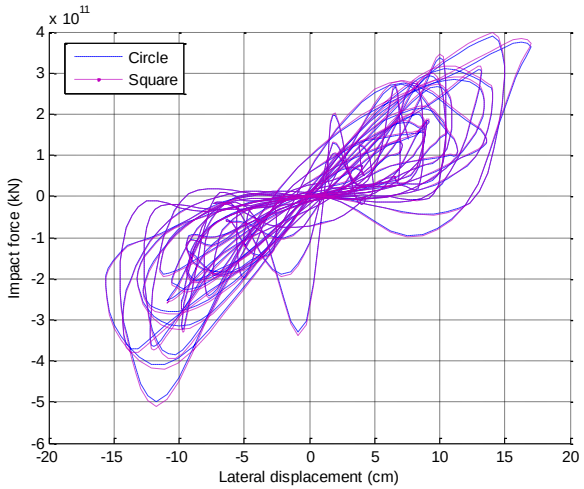

Figure 9. Hysteresis loop of bumper with the same contact area but different shapes.

The analyses of rubber bumpers indicate that the increase of the thickness of bumpers with the same volume significantly decreases impact force and also dissipated energy. It should be also underlined that circle shape of bumper provide an economy benefit (usage of material sharply decreased compared to square model). As it can be seen in Figure 10a, value of peak impact forces determined for square shape model are much more greater than in the case of circle one. For example, keeping the same plan dimensions of the models: b=6 cm (b- width of square model) and r=3 cm (r - radius of circle model), the value of peak impact force is $12.87*10^{12}$ kN and $6.54*10^{12}$ kN, respectively. On the other hand, using circle model with the volume of 3125 cm^3, the peak impact force when r=3 cm is shown about $4.39 \cdot 10^{13}$ kN, which is $3.3 \cdot 10^{13}$ kN, $2.54 \cdot 10^{13}$ kN and $1.76 \cdot 10^{13}$ kN for the volume of 3437 cm^3, 3750 cm^3 and 4375 cm^3, respectively. Consequently, increasing the volume of circle bumper leads to a decline of peak impact force during seismic excitation which can be observed in Figure 10b.

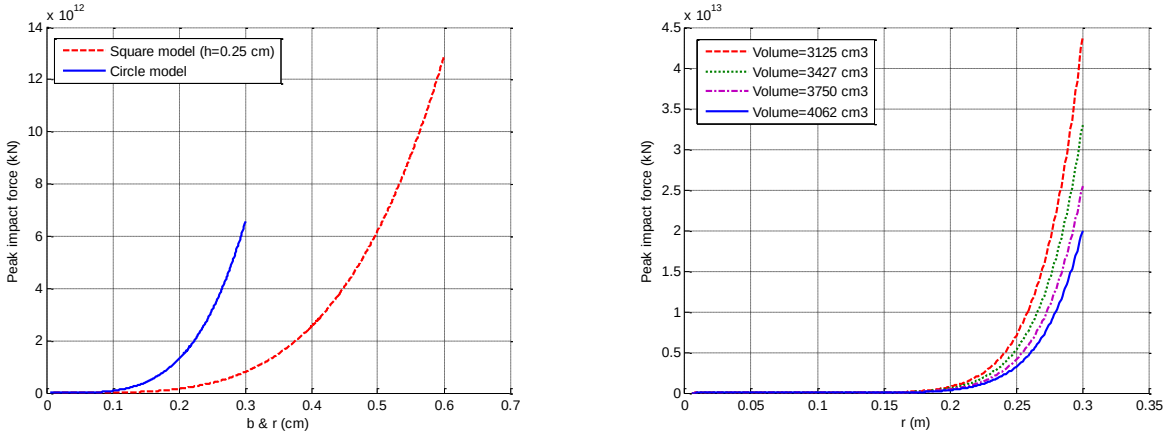

(a) (b)

Figure10. Peak impact force of a) different value of thickness with same dimension and b) different volume of circle model

3.6 Determination of structural damage

Final investigation was devoted to determination of structural damage based on two equations for calculating damage index. This index is one of the most important parameter describing the effect of kinematic and cyclic ductility and also dissipated energy during seismic excitation. Increasing value of damage index, confirmed that the building can be destroyed or collapsed.

The first evaluated damage index depends significantly on the dissipated energy, E_D, yield strength, F_y, peak lateral displacement, δ_y, and also ductility, μ, and can be expressed by the following formula [43]:

$$D_{Index-F} = \frac{E_D}{F_y.\delta_y.(\mu - 1)} \tag{5}$$

Another equation describing determination of damage was suggested by Park et al [44]. It demonstrates structural damage in zone of peak dynamic response which can calculated by:

$$D_{Index-P} = \frac{\delta_{\max}}{\delta_u} + \frac{\beta}{F_y \delta_u} \int dE \tag{6}$$

Where $\delta_{\max}$ and δ_u are the peak displacement and ultimate displacement, respectively. β is also an index parameter, which is recommended to be 0.05 to 0.35. In order to describe the value of capture damage, it can be assumed that $D_{Index} < 0.2$ is a negligible damage, $D_{Index} < 0.4$ denotes a repairable damage, $D_{Index} < 1$ explains an irreparable damage without collapse and finally, $D_{Index} > 1$ demonstrates irreversible failure with a failure collapse.

In here, using the reference model, the peak lateral displacements for 3-story and 4-story buildings were considered (see Figure 4a and 4b) with β equal to 0.2 as well as taking $F_y = 1.23 \cdot 10^5$ N and $F_y = 1.38 \cdot 10^7$ N for 4-story and 3-story model, respectively. All inputs collected for both models under El Centro earthquake record were analysed using previously mentioned structural damage equations. Damage index time histories for 3-story (with bumpers) and 4-story (without bumpers) model of buildings according to Fajfar and Park's formulas are presented in Figure 11a and 11b, respectively.

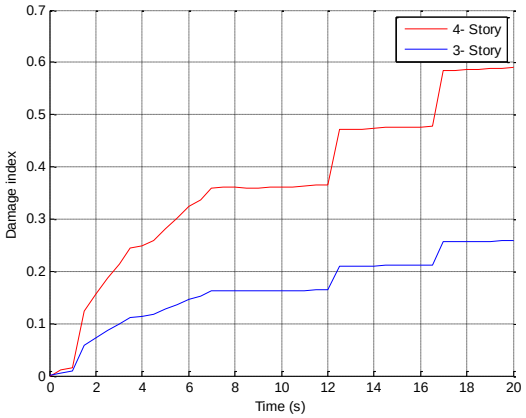

(a)

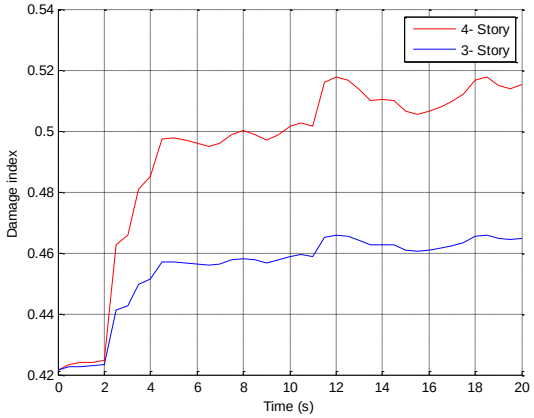

(b)

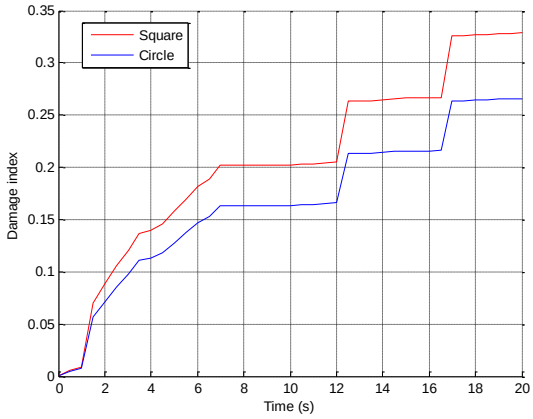

(c)

Figure 11. Damage index time histories for 3-story (with bumpers) and 4-story (without bumpers) model of buildings under El Centro earthquake record according to a) Fajfar; b) Park et al; c) with different shapes of bumpers.

Damage indexes of 3-story model determined using Fajfar formula is equal to 0.254 while in the case of Park's equation it is 0.462 (compare Figure 11a and 11b).Considering the 4-story model the following values of damage indexes are observed: 0.594 and 0.519 using Fajfar and Park et al formulas, respectively. In fact, the results of damage index illustrates that rubber bumper is able to decline the failure risk as have been depicted for both structural damages. All damage indexes for both models are $0.4 < D_{Index} < 1$, which shows an irreparable damage range for models during collisions. In Figure 11c the difference in value of damage indexes in the case of application rubber bumpers with the square and circle shape is shown. Calculating this value for 3-story model, using Fajfar formula they indicate 0.254 and 0.342 for circle and square shapes, respectively.

In order to confirm the effectiveness of application of rubber bumpers in controlling buildings during seismic excitations, one 3- story and one 4- story model of building without any bumpers were modelled and analysed using previously described parameters of models and earthquake record. Damage index time histories for both models without bumpers calculated according to Fajfar and Park's equations are presented in Figure 12a and 12b, respectively.

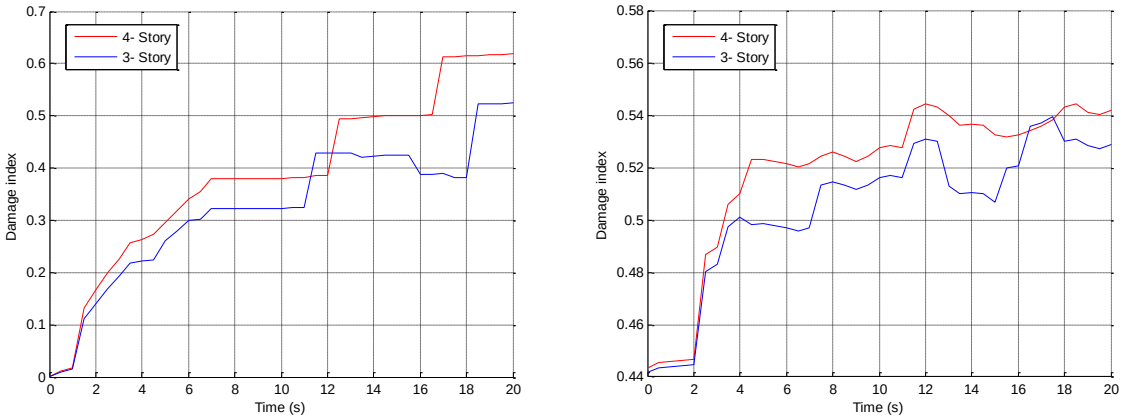

(a) (b)

Figure 12. Damage index time histories for 3- and 4- story model of buildings without rubber bumpers under El Centro earthquake record base on a) Fajfar; b) Park et al.

As it is obviously seen, removing rubber bumpers have normally increased value of damage indexes. It confirmed that application of rubber bumpers has a significant influence on structure's response under earthquake excitations. The final damage index determined using Fajfar formula was equal to 0.254 for 3-story model equipped with rubber bumpers and it significantly increased to 0.521 (more than two times) while those elements were removed.

3.7 Application of circle shape rubber bumpers under different earthquake records

Due to the huge economic aspects of using circle shape of rubber bumpers, dynamic response of these type of elements under earthquake excitations have been considered in the last part of the study. Four different earthquake records were taken into account: Tabas (1975), Parkfield (1966), Kobe (1995) and San Fernando (1971) with peak ground accelerations equal to 817 cm/s^2, 462 cm/s^2, 344 cm/s^2 and 1202 cm/s^2, respectively. The reference model (for 3 and 4-story building) was investigated using different parameters. In Figure 12 lateral displacement time histories obtained under Tabas, Parkfield, Kobe and San Fernando earthquakes are presented.

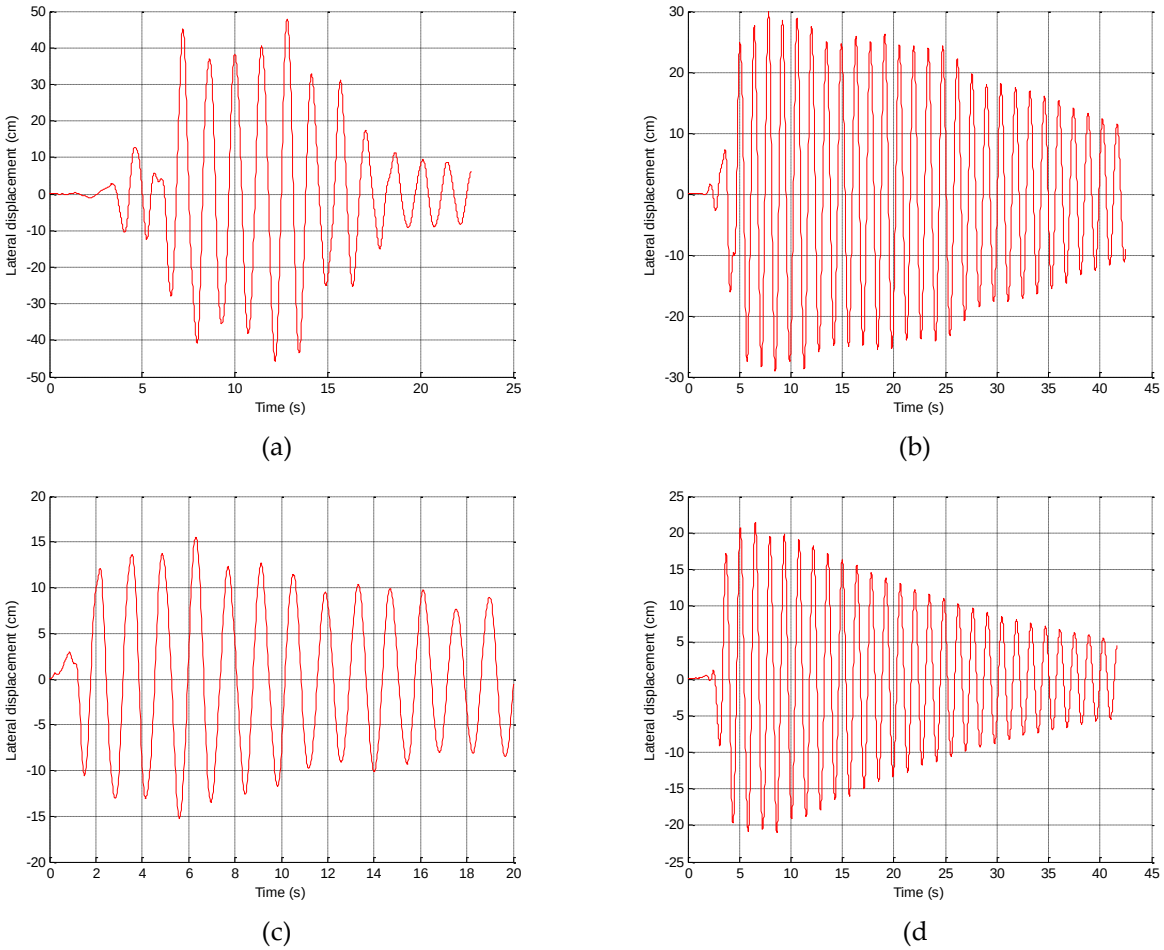

Figure 13. Lateral displacement time history of story no.3 during earthquake records: a) Tabas; b) Parkfield; c) Kobe; d) San Fernando.

In can be seen from Figure 13 that peak lateral displacement of top story of 3-story model of building is equal to 47.21 cm, 29.8 cm, 15.07 cm and 20.95 cm under Tabas, Parkfield, Kobe and San Fernando earthquake records, respectively. In Figure 14 lateral hysteresis loop of rubber bumper obtained under Tabas, Parkfield, Kobe and San Fernando earthquakes are presented.

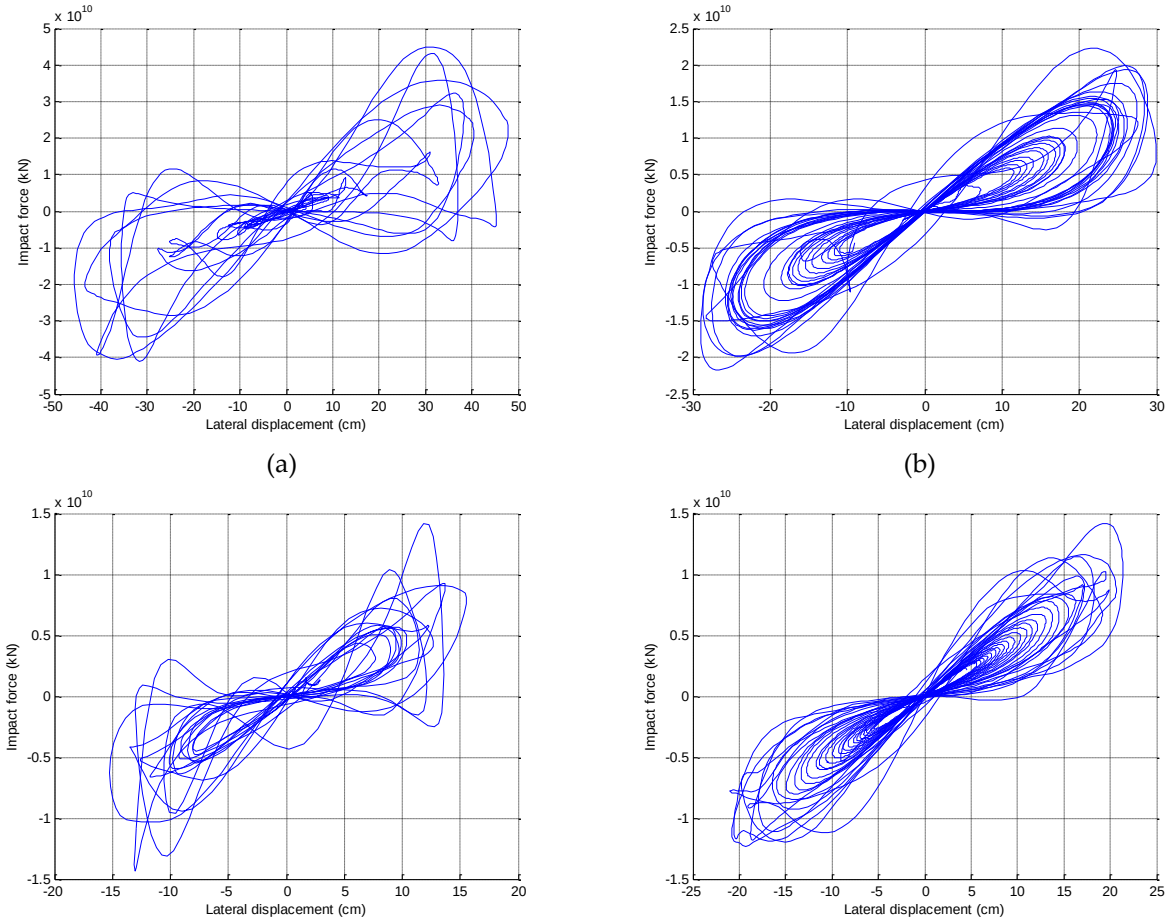

Figure 14. Hysteresis loop of rubber bumper under different earthquake records a) Tabas, b) Parkfield c) Kobe and d) San Fernando

The maximum impact force of top story determined in 3-story model when both models were collided with each other is calculated to be $4.52 \cdot 10^{10}$ kN.cm, $2.25 \cdot 10^{10}$ kN.cm, $1.42 \cdot 10^{10}$ kN.cm and $1.48 \cdot 10^{10}$ kN.cm for Tabas, Parkfield, Kobe and San Fernando earthquake records, respectively.

3.7.1 Circle bumper characterized by the same volume but different contact zone

In this part of the investigate different cross-sectional area of circle shaped bumpers with the same volume have been considered. Following values of radiuses *r* were analysed: 1.35 cm, 1.38 cm, 1.41 cm and 1.44 cm, which provides a slight increase in the thickness of bumpers. Kobe earthquake records have been selected to evaluate the effect of contact zone area in field of

impact force and also dissipated energy. The results obtained from this analysis are presented in Figure 15.

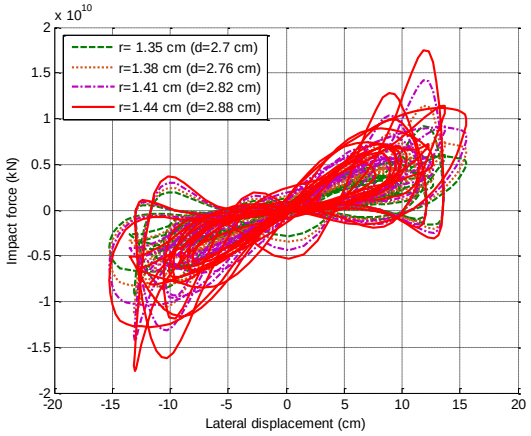

Figure 15. The results for Kobe earthquake record with different area of contact zone

It can be seen from Figure 15 that by increasing the value of radius and also the cross-sectional area of contact zone but keeping the same volume of bumpers, the value of thickness is naturally decreased. For example, the impact forces equal to $9.45 \cdot 10^9$ kN and $1.77 \cdot 10^{10}$ kN were obtained for r=1.35 cm and r=1.44 cm, which confirms increase by about 87%. Consequently, impact force and dissipated energy are increasing when cross-sectional area of contact zone increase. In fact, decreasing the value of thickness causes significant grown in the value of impact force and subsequently, dissipated energy during collision between two model of buildings.

3.7.2 The effect of using different number of circle bumpers

In the next round of the study, the influence of number of bumpers was numerically investigated by using one, two, four and eight bumpers. The analysis was still focused on story no. 3 and Tabas earthquake record were used. The plan dimensions of the bumper was characterized by radius r=1.38 cm. The results of evaluation are shown in Figure 16, which illustrates sharp decrease in field of impact force with increasing number of bumpers.

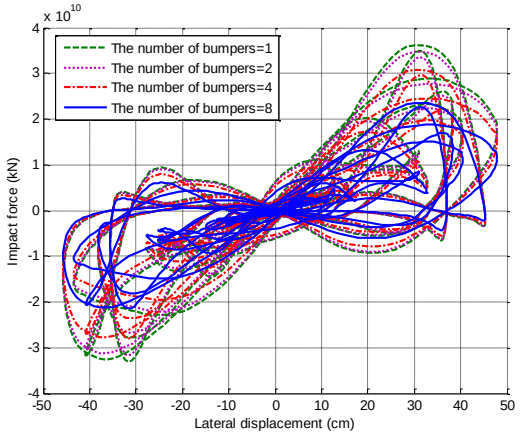

Figure 16. The results for Tabas earthquake record with different number of bumpers.

For instance, the peak impact forces were determined and they were equal to $3.73 \cdot 10^9$ kN, $3.58 \cdot 10^9$ kN, $3.12 \cdot 10^9$ kN and $2.38 \cdot 10^9$ kN for the model where one, two, four and eight bumpers were used, respectively. The results of investigation demonstrate that increasing the number of bumpers decreases impact force so as to increase the compressive strain of the bumpers.

4. Conclusion

In this paper, the optimum shapes and dimensions of rubber bumpers were investigated in order to reduce negative effects of pounding between buildings during seismic excitations. A model of 3-story building equipped with rubber bumpers and a model of 4-story building were generated. Rubber bumpers were attached at each level of story to absorb energy during impact. Several different shapes and dimensions of bumper elements were numerically investigated so as to find the most effective ones. Firstly, rubber bumpers characterized by the same volume but different plan dimensions have been considered. It has been proved that increasing the value of bumper thickness basically decreases impact force and dissipated energy. In fact, the same volume of bumpers has specifically shown various responses in field of impact force and energy dissipation. Additionally, rubber bumpers characterized by the same responses but different dimensions have been analysed. The results of such investigation demonstrate that by increasing the value of plan dimensions of square shape bumpers, the value of thickness is increased to obtain similar responses during impact between models. Next consideration has been focused on rubber bumpers with the same cross-sectional area but different thickness. The results of this study shows, that by decreasing the thickness of bumpers, impact force and dissipated energy significantly increased. Also, circle shape was found to be more effective, comparing to the square one, from the point of the level of impact force, energy dissipation. Consequently, increasing the volume of circle bumper leads to a decline of peak impact force during seismic excitation. Final investigation was devoted to determination of structural damage based on two equations for calculating damage index. It was also demonstrated that the building with rubber bumper has a much smaller damage index than the structure without bumper elements. It confirmed that application of rubber bumpers has a significant influence on structure's response under earthquake excitations.

The presented paper has been limited to the analysis of pounding between 3-story and 4-story concrete buildings. The limitation has also concerned the adopted gap distance, mechanical properties of rubber bumpers, studied earthquake, etc. Therefore, further research is needed to be conducted so as to verify the effectiveness of rubber bumpers in reducing the negative effects of earthquake-induced pounding between various types of buildings under different configurations.

REFERENCES

1- Grębowski K. Cable-stayed cantilever structures as an expat of unique application in the construction of a building located in seismic area – an author's project of multifunctional building in Lisbon, Portugal. International Journal of Applied Mechanics and Engineering, 2015; 20(4): 805-816.
2- Grębowski K & Zielińska M. Dynamic analysis of historic railway bridges in Poland in the context of adjusting them to pendolino trains. International Journal of Applied Mechanics and Engineering, 2015; 20(2): 283-287.

3- Anagnostopoulos SA & Karamaneas CE. Use of collision shear walls to minimize seismic separation and to protect adjacent buildings from collapse due to earthquake-induced pounding. Earthq. Eng. Struct. Dyn., 2008; 37(12): 1371-1388.
4- Elwardany H, Seleemah A, Jankowski R, El-Khoriby S. Influence of soil-structure interaction on seismic pounding between steel frame buildings considering the effect of infill panels. Bulletin of Earthquake Engineering, 2019; 17(11): 6165-6202.
5- Rezaei H, Moayyedi SA, Jankowski R. Probabilistic seismic assessment of RC box-girder highway bridges with unequal-height piers subjected to earthquake-induced pounding. Bulletin of Earthquake Engineering, 2020; 18(4): 1547-1578.
6- Liu Ch, Fang D, Zhao L. Reflection on earthquake damage of buildings in 2015 Nepal earthquake and seismic measures for post-earthquake reconstruction. Structures, 2021; 30: 647-658.
7- Khatami SM, Naderpour H, Mortezaei A, Nazem Razavi SM, Lasowicz N, Jankowski R. Effective Gap Size Index for Determination of Optimum Separation Distance Preventing Pounding between Buildings during Earthquakes. Appl. Sci., 2021; 11(5): 2322.
8- Jia HY, Lan XL, Zheng SX, Li LP, Liu ChQ. Assessment on required separation length between adjacent bridge segments to avoid pounding. Soil Dynamics and Earthquake Engineering, 2019;120: 398-407.
9- Barros RC and Khatami SM. Damping Ratios for Pounding of Adjacent Buildings and Their Consequence on the Evaluation of Impact Forces by Numerical and Experimental Models. Mecânica Experimental, 2013; 22: 119-131.
10- Dogruel S. Application of genetic algorithms for optimal aseismic design of passively damped adjacent structures. Individual Study, State University of New York at Buffalo, United States, 2005.
11- Braz C, Barros RC. Semi-active Vibration Control of Buildings using MR Dampers: Numerical and Experimental Verification. In: 14th Earthquake Conference on Earthquake Engineering, Macedonia, URL, 2010.
12- Lopez-Garcia D and Soong TT. Evaluation of current criteria in predicting the separation necessary to prevent seismic pounding between nonlinear hysteretic structural systems. Engineering Structures, 2009; 31(5): 1217-1229.
13- Garcia DL. Separation between adjacent non-linear structures for prevention of seismic pounding. In: Proceedings of 13th World Conference on Earthquake Engineering, Vancouver, Canada, 2004.
14- Zhang WS and Xu YL Dynamic characteristics and seismic response of adjacent buildings linked by discrete dampers. Earthq. Eng. Struct. Dyn., 1999; 2: 1163-1185.
15- Matsagar VA and Jangid RS. Viscoelastic damper connected to adjacent structures involving seismic isolation. J. Civil Eng. Manage., 2005; 11(4): 309-322.
16- Westermo BD. The dynamics of interstructural connection to prevent pounding. Earthq. Eng. Struct. Dyn., 1989; 18: 687–699.
17- Kasai K, Jeng V, Patel PC, Munshi JA, Maison BF. Seismic pounding effects—survey and analysis. In: Proceedings of the 10th World Cconference on Earthquake Engineering, Madrid, Spain 19–24 July 1992; 7: 3893–3898.
18- Stręk AM, Lasowicz N, Kwiecień A, Zając B, Jankowski R. Highly Dissipative Materials for Damage Protection against Earthquake-Induced Structural Pounding. Materials, 2021; 14(12): 3231.
19- Kelly J.M. Earthquake-resistant design with rubber. London: Springer; 1993.
20- Falborski T, Jankowski R, Kwiecień A. Experimental study on polymer mass used to repair damaged structures. Key Eng. Mater., 2012; 488-48: 347-350.
21- Falborski T, Jankowski R. Polymeric bearings – a new base isolation system to reduce structural damage during earthquakes. Key Eng. Mater., 2013; 569-570: 143-150.
22- Jankowski R. Pounding between superstructure segments in multi-supported elevated bridge with three-span continuous deck under 3D non-uniform earthquake excitation. J. Earthq. Tsunami, 2015; 9(4): 1550012.
23- Liu C, Yang W, Yan Z, Lu Z, Luo N. Base Pounding Model and Response Analysis of Base-Isolated Structures under Earthquake Excitation. Appl. Sci., 2017; 7: 1238.
24- Liu C, Fang D, Yan Z. Seismic Fragility Analysis of Base Isolated Structure Subjected to Near-fault Ground Motions. Periodica Polytechnica Civil Engineering, 2021; 65(3): 768–783, 2021.
25- Khatami SM, Naderpour H, Nazem Razavi SM, Barros RC, Jakubczyk-Gałczyńska A, Jankowski R. Study on Methods to Control Interstory Deflection. Geoscience, 2020; 10(75): 10.3990.
26- Naderpour H, Naji N, Burkacki D, Jankowski R. Seismic response of high-rise buildings equipped with base isolation and non-traditional tuned mass dampers. Appl. Sci., 2019; 9(6): 1201.

27- Zhao N, Lu Ch, Chen M, Luo N. Parametric Study of Pounding Tuned Mass Damper Based on Experiment of Vibration Control of a Traffic Signal Structure. Journal of Aerospace Engineering, 2018; 31(6).
28- Panayiotis C, Polycarpou P, Komodromos P. Numerical investigation of potential mitigation measures for pounding of seismically isolated building. Earthquake and Structures, 2011; 2(1): 1-24.
29- Anagnostopoulos SA. Pounding of buildings in series during earthquakes. Earthq. Eng. Struct. Dyn., 1988; 16: 443–456.
30- Polycarpou PC, Komodromos P, Polycarpou AC. A nonlinear impact model for simulating the use of rubber shock absorbers for mitigating the effects of structural pounding during earthquakes. Earthq. Eng. Struct. Dyn., 2013; 42: 81–100.
31- Abdel Raheem SE. Mitigation measures for earthquake induced pounding effects on seismic performance of adjacent buildings. Bull. Earthq. Eng., 2014; 12: 1705–1724.
32- Khatami SM, Naderpour H, Mortezaei AR, Sharbatdar AR, Lasowicz N, Jankowski R. The Effectiveness of Rubber Bumpers in Reducing the Effect of Earthquake-Induced Pounding between Base-Isolation Buildings. Appl. Sci., 2021; 12: 4971.
33- Al-Fahdawi OA, Barroso LR, Soares RW. Utilizing the adaptive control in mitigating the seismic response of adjacent buildings connected with MR dampers. In: Proceedings of the Annual American Control Conference (ACC), Milwaukee, WI, USA, 27–29 June 2018, 912–917.
34- Al-Fahdawi OA, Barroso LR. Adaptive neuro-fuzzy and simple adaptive control methods for full three-dimensional coupled buildings subjected to bi-directional seismic excitations. Eng. Struct., 2021; 232: 111798.
35- Matsagar VA, Jangid RS. Viscoelastic damper connected to adjacent structures involving seismic isolation. J. Civ. Eng. Manag., 2005; 11: 309–322.
36- Sołtysik B, Falborski T, Jankowski R. Preventing of earthquake-induced pounding between steel structures by using polymer elements – experimental study. Procedia Engineering, 2017; 199: 278-283.
37- Jankowski R, Wilde K, Fujino Y. Reduction of pounding effects in elevated bridges during earthquakes. Earthquake engineering & structural dynamics, 2000; 29(2): 195-212.
38- Naderpour H, Barros RC, Khatami SM, Jankowski R. Numerical Study on Pounding between Two Adjacent Buildings under Earthquake Excitation. Shock. Vib., 2016; 2016: 1504783.
39- Kajita Y, Kitahara T, Nishimoto N. Estimation of maximum impact force on natural rubber during collision. In: Proceedings of 1st European Conference on Earthquake Engineering and Seismologhy (ECEES), 2016; Geneva, Switzerland.
40- Li B & Yang Z. Assessment of spectrum-matched time histories for floor response spectra generation. Structures, 2022; 38.
41- Li B, Zhen C, Zhongdong D. Generating spectrum-matched bidirectional time histories using Hilbert-Huang Transform. Journal of Building Engineering, 2022; 105033.
42- Chopra A. K.: Dynamics of Structures: Theory and Applications to Earthquake Engineering. Pearson Education Limited, USA 2019.
43- Fajfar P. Equvalent ductility factors, taking into account low-cycle fatigue. Earthquake Eng. Struct. Dynam., 1992; 21: 837-484.
44- Park YJ, Ang AHS, Wen YK. Seismic damage analysis of reinforced concrete building. J. Struct. Eng., 1985; 111: 740-757.